Volume 53
Number 31
21 August 2024
Pages 12801-13218

Dalton Transactions

An international journal of inorganic chemistry

rsc.li/dalton

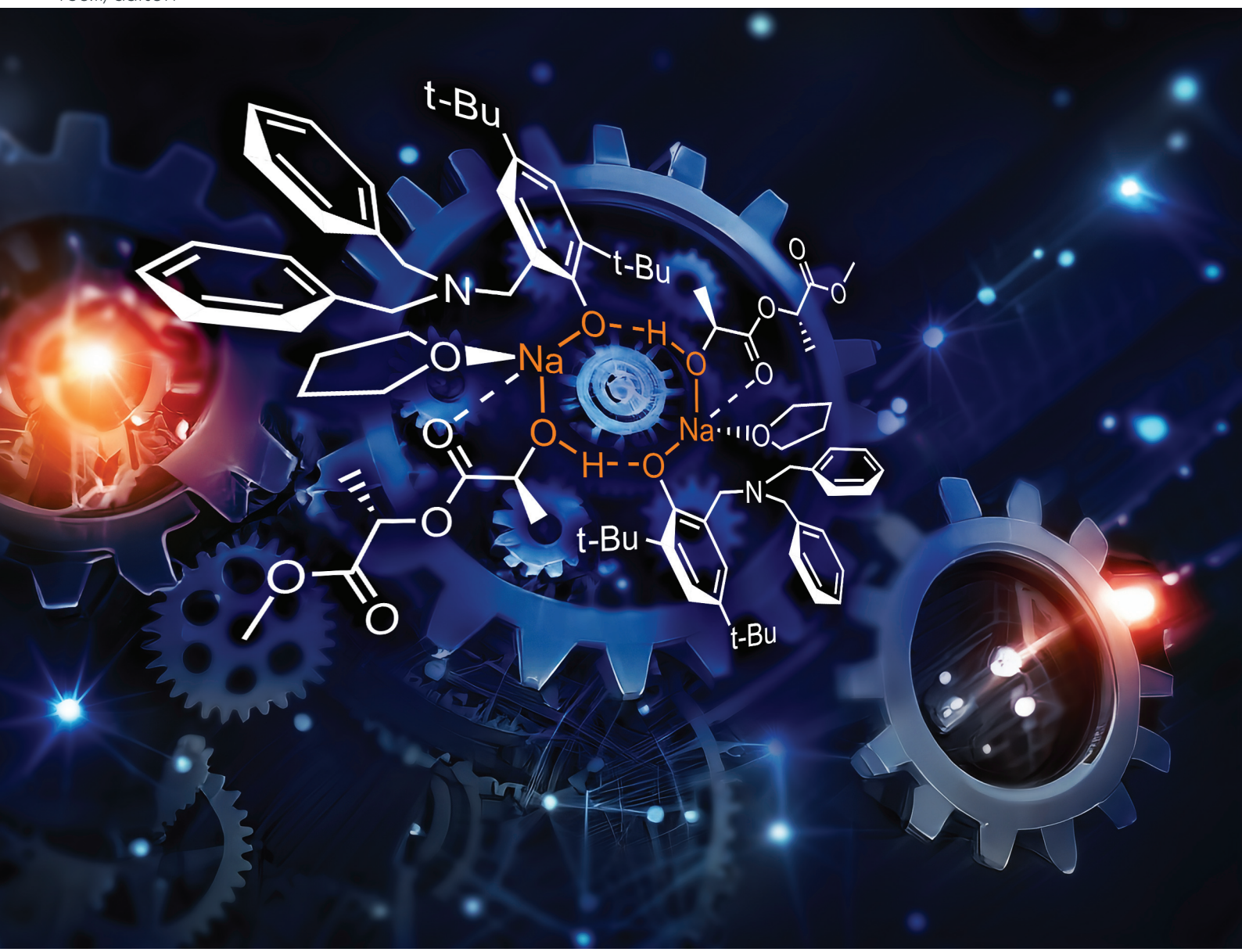

ISSN 1477-9226

ROYAL SOCIETY OF CHEMISTRY

PAPER

Jolanta Ejfler *et al.*

Structural subtleties and catalytic activity of sodium aminophenolate complexes in polylactide degradation: towards sustainable waste management solutions

Dalton Transactions

ROYAL SOCIETY OF CHEMISTRY

PAPER

View Article Online
View Journal | View Issue

Cite this: *Dalton Trans.*, 2024, **53**, 12893

Structural subtleties and catalytic activity of sodium aminophenolate complexes in polylactide degradation: towards sustainable waste management solutions†

Edyta Nizioł [a] Aleksandra Marszałek-Harych,[a] Wiktor Zierkiewicz, [b] Łukasz John [a] and Jolanta Ejfler *[a]

This study explores the intricate coordination chemistry of sodium aminophenolate species and their significant role in the depolymerization of polylactide (PLA), offering novel insights into catalytic degradation processes. By examining sodium coordination entities, including dimers and larger aggregates such as tetramers, we reveal how structural modifications, particularly the manipulation of steric hindrances, influence the formation and stability of these complexes. The dimers, characterized by a unique four-center core (Na–O–Na–O), serve as a foundational motif, which is further elaborated to obtain complexes with varied coordination environments through strategic ligand design. Our research delves into the lability of the amino arm in these complexes, a critical factor that facilitates the coordination of PLA to the sodium center, thereby initiating the depolymerization process. Moreover, DFT studies have been pivotal in identifying the most energetically favorable structures for catalysis, highlighting a distinct preference for an eight-membered ring motif stabilized by intramolecular hydrogen bonds. This motif not only enhances the catalyst's efficiency but also introduces a novel structural paradigm for sodium-based catalysis in PLA degradation. Experimental validation of the theoretical models was achieved through NMR spectroscopy, which confirmed the formation of the active catalyst forms and monitored the progress of PLA degradation. The study presents a comprehensive analysis of the influence of ligand structure on the catalytic activity, underscoring the importance of the eight-membered ring motif. Furthermore, we demonstrate how varying the steric bulk of substituents on the amino arm affects the catalyst's performance, with benzyl-substituted ligands exhibiting superior activity. Our findings offer a profound understanding of the structural factors governing the catalytic efficiency of sodium aminophenolate complexes in PLA degradation. This research not only advances the field of coordination chemistry but also presents a promising avenue for the development of efficient and environmentally friendly catalysts for polymer degradation.

Received 30th April 2024,
Accepted 25th May 2024

DOI: 10.1039/d4dt01270d

rsc.li/dalton

Introduction

The management of environmentally degrading polymer wastes is a global issue.[1–3] Environmental devastation processes affect both polymer materials, including the most persistent ones such as durable, degradation-resistant polyolefins, as well as those perceived as potentially safer, such as materials based on (bio)degradable polymers.

In processes depicted in circular models, such as the polylactide (PLA) loop, materials based on this polymer may potentially undergo degradation in the environment. However, additives improving degradation profile, modifying functional properties, or utility parameters may accumulate and, in the long term, affect environmental degradation. The range of applications for PLA-based materials is vast, from environmentally friendly products with a short lifespan to materials used in advanced technologies in medicine and pharmacy.[4–12] PLA production is based on green technology relying on the catalytic ROP (ring-opening polymerization) process of lactide.[13]

As part of basic research, catalysts based on biometals (*e.g.*, Na,[14–26] Mg,[26–29] Zn[28–33]) have been obtained for several years as alternatives to the commercial non-ecological catalyst $Sn(Oct)_2$. Despite the fact that PLA production meets many

[a]*Faculty of Chemistry, University of Wrocław, 14 F. Joliot-Curie, 50-383 Wrocław, Poland. E-mail: jolanta.ejfler@uwr.edu.pl*
[b]*Faculty of Chemistry, Wrocław University of Science and Technology, 27 Wybrzeże Wyspiańskiego, 50-370 Wrocław, Poland*

† Electronic supplementary information (ESI) available. See DOI: https://doi.org/10.1039/d4dt01270d

requirements proposed for green processes, the reverse process of catalytic degradation is poorly understood. Examples of degradation processes include hydrolysis[34–38] and alcoholysis.[39–49] The portfolio of investigated catalysts includes simple inorganic compounds,[46–50] organic compounds,[44,45] and ionic liquids.[38–41,51,52] It seems obvious that this set should include metal coordination compounds that are active in the ROP process of lactides, but this aspect has only emerged in recent years, generally for magnesium and zinc compounds.[32,53–61] The first example was a homoleptic zinc aminophenolate, where we demonstrated that this catalyst exhibits bifunctional characteristics, being active in both the lactide polymerization process and PLA degradation, although the latter process is significantly less efficient.[32] Over the following years, we searched for a candidate that would dominate this second process, which is crucial from the perspective of environmental protection and waste management. In our latest work, we characterized the only catalyst for PLA degradation to date based on a sodium complex.[62]

The full analysis and development of detailed guidelines for designing catalysts for the degradation of cyclic esters *via* a controlled process is the subject of this manuscript. We present an analysis of the motif structure of the active form of sodium catalyst, two versions of the degradation reaction mechanism of PLA on a set of complexes stabilized by aminophenolate ligands modified within the amino arm. The theoretical DFT modeling studies were experimentally verified by testing the obtained catalysts in PLA degradation reactions. The perfect convergence of theoretical and experimental studies indicates that new active catalysts can be designed based on the proposed scheme.

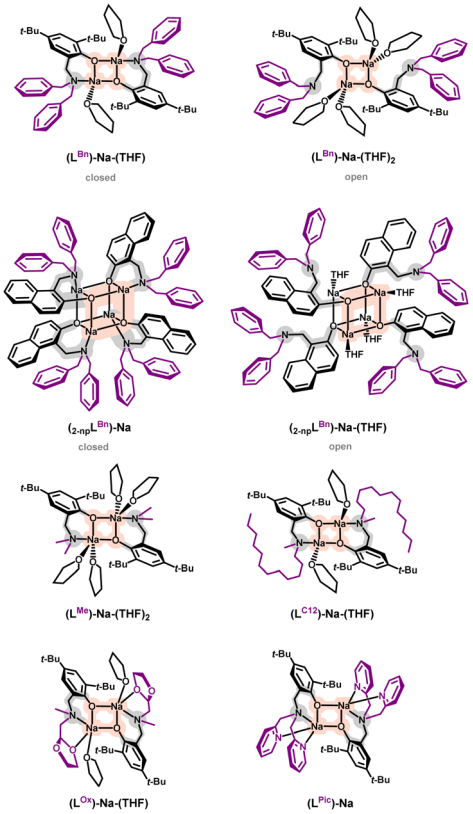

Fig. 1 Examples of sodium coordination entities containing aminophenolate/naphthalenolate ligands.

Results and discussion

Structural nuances of sodium aminophenolates

Coordination entities of sodium with aminophenolate ligands form dimers in which phenolate oxygen atoms serve as bridges connecting sodium ions, nitrogen atoms are located in terminal positions, the coordination sphere is complemented by donor atoms of the amino arm, and solvent molecules (*e.g.*, THF). Such a structural motif is typical for ligands based on functionalized phenols.[28–33] By controlling steric hindrances, larger aggregates such as tetramers can be obtained, influencing the lability of the amino arm (Fig. 1).[62,63]

An example of "twin" compounds with a labile amino arm are dimers (L^{Bn})-Na-(THF) (closed form) and (L^{Bn})-Na-$(THF)_2$ (open form), where the vacant coordination site after breaking the Na–N bond is occupied by a THF solvent molecule. A significant reduction in steric hindrance from benzyl groups in the motif of the compound (L^{Bn})-Na-(THF) to methyl groups allows for the coordination of another solvent molecule, resulting in the structure observed for the compound (L^{Me})-Na-$(THF)_2$. Substituting one methyl group with an oxolane ring in the compound (L^{Ox})-Na-(THF) results in oxygen coordination from this ring instead of the THF molecule. Complete removal of THF molecules can be achieved for a ligand with an amino arm containing two coordinatable substituents, as in the compound (L^{Pic})-Na.

Generally, the structural motif of the dimer is maintained if functionalization occurs within the amino arm with an aromatic core with steric hindrances in *ortho* and *para* positions, effectively blocking further aggregation. Unlocking can be achieved by introducing naphthalene cores where an additional ring mimics the 2D hindrance in these positions, leading to the merging of dimers into tetramers containing "closed" motifs (ligand coordination through oxygen and nitrogen) and "open" motifs (coordination solely through oxygen). However, it should be emphasized that the common structural motif for both dimers and tetramers is a four-center core (Na–O–Na–O), where sodium ions are connected by phenolate oxygen atoms.

The lability of the amino arm is crucial in controlling the reactivity of such compounds, especially when considering their potential applications. Decoordination of the nitrogen atom increases access to the metal center and enables the coordination of other molecules. This lability was the starting point for the application of the compound (L^{Bn})-Na-(THF) as a catalyst for the depolymerization reaction of polylactide (PLA).

The molecular structure in the solid state provides the basis for interpreting spectroscopic data in solution, including analysis of whether a given structural motif is identical to that

determined in the solid state. In the case of sodium aminophenolates, the coordination sphere can undergo transformation due to the planned lability of Na–N bonds, dynamic phenomena in solution, and aggregation into polynuclear systems. However, a constant element is the four-center core (Na–O–Na–O). In applied studies related to catalysis, the foundation often lies in the literature paradigm that defines the structural aspects of the active catalyst's construction. The most enigmatic aspect is usually the coordination mode of the substrate to the active center; in this context, it is worthwhile to support the design of new catalysts using theoretical methods. Such an approach does not always provide definitive solutions but can direct synthesis towards unconventional pathways.

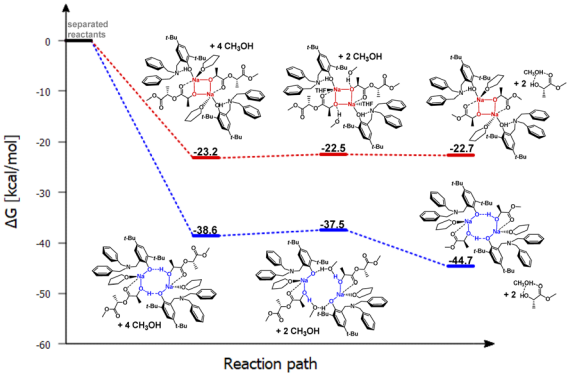

Fig. 3 Relative Gibbs free energies for DFT optimized structures of two proposed versions of the structural motifs of the active catalyst (L^{Bn})-Na-(THF)(PLA) in the PLA degradation reaction.

DFT calculations

The coordination mode of PLA to the sodium complex and the optimal structural motif of the active catalyst form were determined using theoretical DFT methods.

The dimeric sodium complex, where the aminophenolate ligand (open form) is bound to the metal center *via* phenolate oxygen, exhibited the lowest energy. Meanwhile, PLA chains form successive bridges between sodium ions, coordinating through the carbonyl oxygen and hydroxyl groups stabilized by hydrogen bonds Ph/O···H/PLA (Fig. 2, blue pathway). Methyl lactyl lactate (Me-LLA) was used as a model for PLA in the calculations. Calculations were also performed for the pentamer (5-PLA-Me), clearly demonstrating that the process is spontaneous.[62]

Polymer degradation requires adding PLA to the catalyst, one polymer chain per active center [Na], then after forming the complex (Na-PLA), applying alcohol to cleave the PLA chain in a stoichiometry of ROH/mer = 4/1.[62] Full analysis of the process also requires verification of the second version while maintaining the complex structure resulting from the analysis of sodium coordination compounds with aminophenols, namely the four-center motif (Na–O–Na–O) (Fig. 2, red pathway). The energy chart for these two variants is shown in Fig. 3; in this study, we optimized the process for isotactic P*L*LA (in the text, P*L*LA will be referred to as PLA).

In the context of theoretical considerations, both the mechanism based on the red and blue variants are probable, as in both cases the reactions are spontaneous. However, the energy difference between these pathways, particularly for the first stage, which amounts to 15.4 kcal mol^{-1}, indicates that the version based on the model with an eight-membered ring stabilized by intramolecular hydrogen bonding is decidedly more preferred. This solution, being unique, points to a completely new and never-before-proposed structural motif of the active form of the catalyst.

In the next stage, it was crucial to verify whether steric factors and the coordination properties of the ligand could influence the structure of the active form of the catalyst, which should be evident in experimental studies illustrating the actual catalytic activity of sodium aminophenolates. For this purpose, previously obtained sodium compounds containing aminophenolate ligands with the same aromatic core and substituents on the amino arm varying in terms of steric hindrance or the presence of donor atoms were used (Fig. 1). It was also significant in this selection that crystal structures were determined for each compound in this set.

In the theoretical studies, two variants of the structure of the active form of the catalyst were optimized, containing motifs with a four-membered and an eight-membered ring.

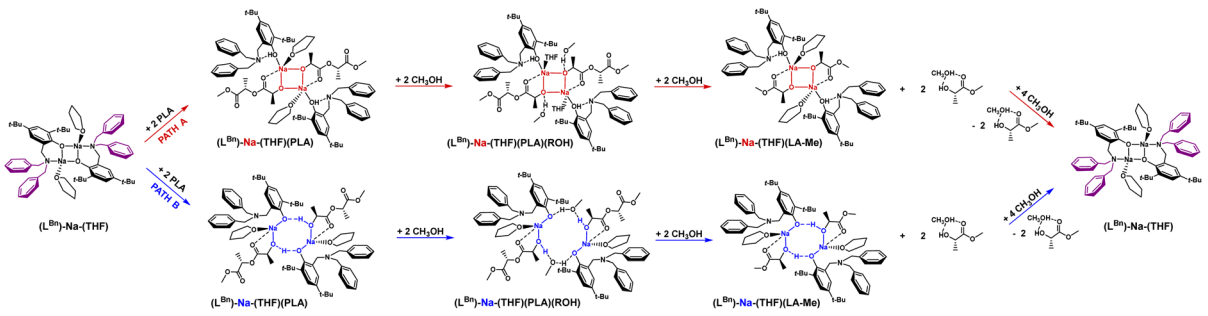

Fig. 2 Proposed two versions of the structural motifs of the active sodium catalyst (L^{Bn})-Na-(THF)(PLA) in the PLA degradation reaction: red pathway – a four-center motif Na–O–Na–O; blue pathway – an eight-membered ring stabilized by intramolecular hydrogen bonds Ph/O···H/PLA.

The radical reduction of steric hindrance from benzyl to methyl results in the coordination of another molecule of the solvent THF to the sodium ion. Nevertheless, this does not significantly affect the structure of the active catalyst in the degradation process of PLA, and for the compound (L^{Me})-Na-$(THF)_2$, the structural motif with the eight-membered ring is still preferred (Fig. 4 and 5). It is worth noting that in this case, the energy difference for the first stage, *i.e.*, the coordination of the polymer chain to the metal center between the two considered proposals, is significantly greater than for the complex (L^{Bn})-Na-(THF). Exposing the center maintains solvent molecules within the metal's coordination sphere, which may lead to reduced reactivity in the degradation process of PLA. In the case of the version with a four-membered ring, the sodium ion is fully coordinated, significantly hindering subsequent reactions in the catalytic degradation cycle.

Another modification of the amino arm involved replacing one methyl substituent with a long alkyl chain (L^{C12})-Na-(THF). Such a solution, similar to (L^{Bn})-Na-(THF), results in the coordination of only one THF molecule to the active center. In this case, theoretical studies also indicate that the eight-membered ring is preferred. However, the very small energy difference between the proposed variants in the first stage of the reaction, amounting to 8.6 kcal mol^{-1}, may suggest that structures with both four- and eight-membered active centers will be present in the solution (Fig. 6 and 7). However, the version with a four-membered ring may lead to the termination of the reaction after the introduction of the alcohol.

Manipulating steric hindrance in the studied examples of sodium compounds indicates the same trend, namely the stabilization of compounds with an eight-membered ring. The compound with benzyl substituents is the most energetically favorable. The introduction of an additional donor atom on the amino arm undoubtedly must alter the way metal centers coordinate after coordinating the PLA chain.

Substituting pyridyl rings instead of benzyl rings does not significantly change the steric parameters; however, the nitrogen atoms of this ring coordinate to sodium, displacing the

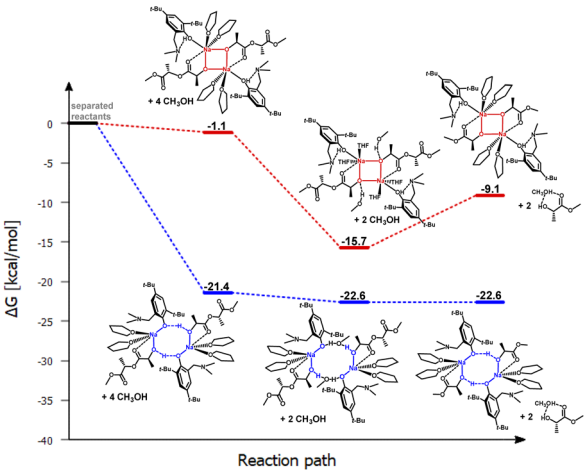

Fig. 5 Relative Gibbs free energies for DFT optimized structures of two proposed versions of the structural motifs of the active catalyst (L^{Me})-Na-$(THF)_2$(PLA) in the PLA degradation reaction.

THF molecule from the structure. Optimization of the structures (L^{Pic})-Na-(PLA) formed during the polymer coordination process revealed an extremely interesting solution, Fig. 8.

The eight-membered ring is preserved, but it gains additional stabilization through the atypical coordination of the nitrogen in the pyridyl ring. Aminophenol coordinates through the phenolic oxygen to one sodium center, while the nitrogen from one substituent coordinates to another sodium ion. The second substituent remains inert. As a result, rings are "bonded" together by the oxygen atoms of phenolic groups and sodium. Similar to previous cases, this model is also preferred in terms of energy considerations for these reaction steps compared to the classical model based on a four-membered ring (Fig. 9). The bond lengths between the sodium ions and the nitrogen atoms of the pyridyl ring after PLA coordination are longer compared to the starting coordination entity, where the ligand's donor atoms coordinate to the same metal center; these bond lengths are respectively 2.64, 2.55, and 2.45, 2.43 Å. Interestingly, after incorporating methanol and

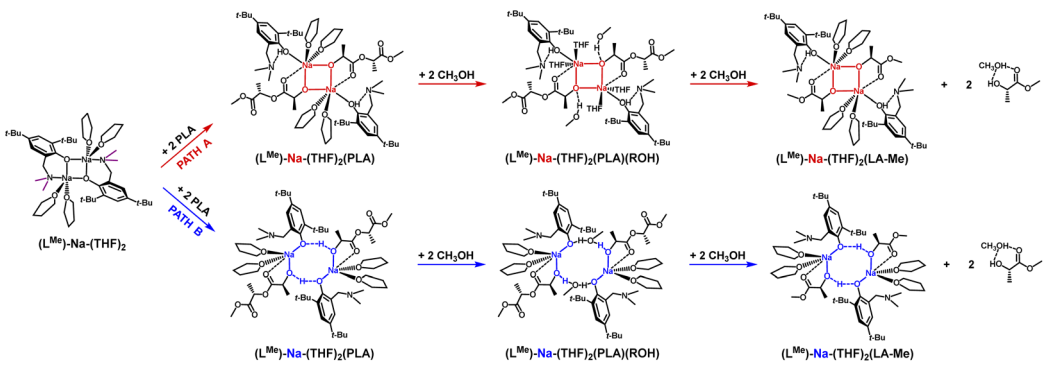

Fig. 4 Two proposed versions of the structural motifs of the active sodium catalyst (L^{Me})-Na-$(THF)_2$(PLA) in the degradation reaction of PLA: red pathway – a four-membered motif Na–O–Na–O; blue pathway – an eight-membered ring stabilized by intramolecular hydrogen bonds Ph/O···H/PLA.

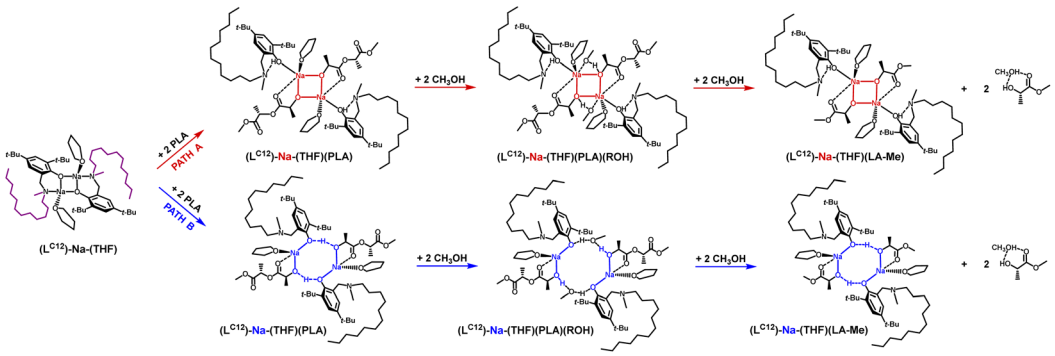

Fig. 6 Two proposed versions of the structural motifs of the active sodium catalyst (L^{C12})-Na-(THF)(PLA) in the degradation reaction of PLA: red pathway – a four-membered motif Na–O–Na–O; blue pathway – an eight-membered ring stabilized by intramolecular hydrogen bonds Ph/O···H/PLA.

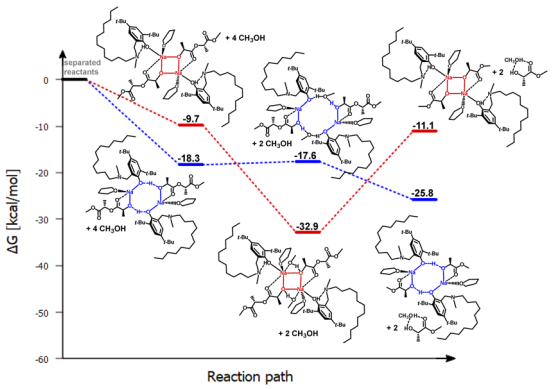

Fig. 7 Relative Gibbs free energies for DFT optimized structures of two proposed versions of the structural motifs of the active catalyst (L^{C12})-Na-(THF)(PLA) in the PLA degradation reaction.

expanding the ring, these bond lengths shorten to 2.48 and 2.46 Å. This fact may indicate that at this stage, there could be stabilization of the structure, which would prevent the transformation of the PLA chain essential for PLA fragmentation. As a result, after coordinating PLA and adding methanol, the reaction may cease.

Analyzing the molecular structure of this compound, it appears that the second of the pyridyl substituents is inert in terms of coordination, but it may pose a steric barrier during further stages of PLA degradation reaction. Therefore, the question arises whether such a motif will also be preserved if the aminophenolate ligand contains only one coordinating substituent. This situation was analyzed for the sodium compound with a ligand containing one low steric hindrance substituent, namely methyl, and the other with an oxolanyl ring containing a donor oxygen atom. The result of this operation is illustrated in Fig. 10 and 11.

The results of DFT studies unequivocally indicate that a dimer with a similar arrangement was obtained, with an eight-membered ring stabilized by bridging with an oxolanyl fragment between two sodium centers; the methyl substituent does not pose a barrier for subsequent stages of depolymerization reaction. However, energy analysis for these two versions suggests that PLA coordination is stabilized by a similar structural motif as in the previous catalysts, *i.e.*, involving an eight-membered ring. The next stage, incorporation of methanol,

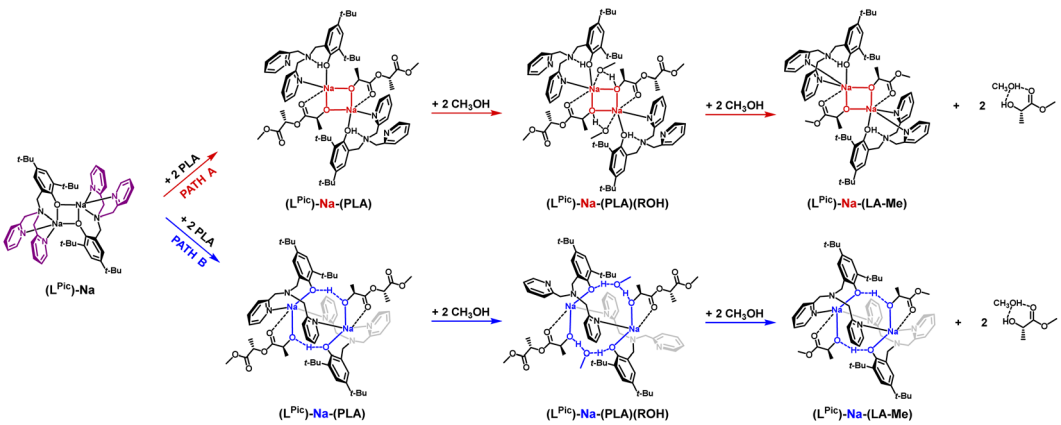

Fig. 8 Two proposed versions of the structural motifs of the active sodium catalyst (L^{Pic})-Na-(PLA) in the degradation reaction of PLA: red pathway – a four-membered motif Na–O–Na–O; blue pathway – an eight-membered ring stabilized by intramolecular hydrogen bonds Ph/O···H/PLA.

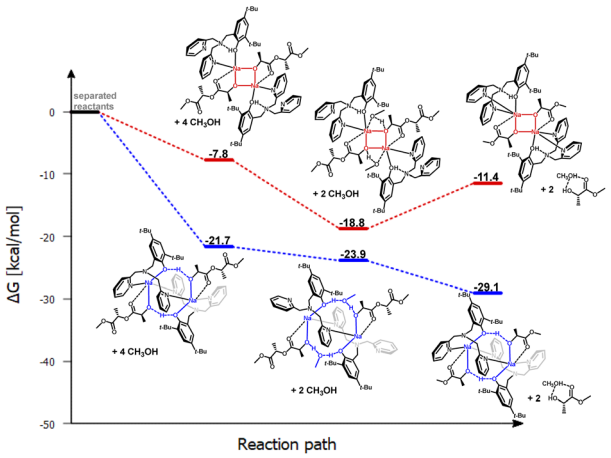

Fig. 9 Relative Gibbs free energies for DFT optimized structures of two proposed versions of the structural motifs of the active catalyst (L^{Pic})-Na-(PLA) in the PLA degradation reaction.

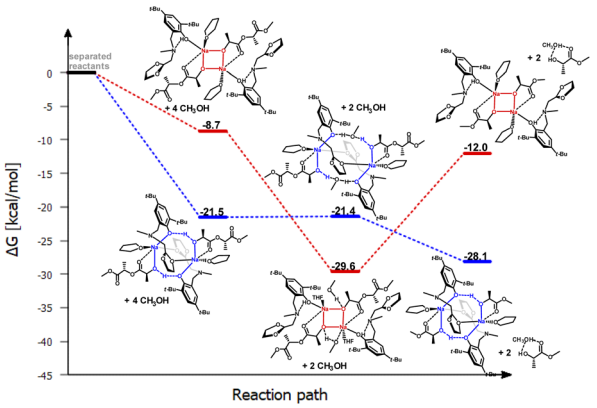

Fig. 11 Relative Gibbs free energies for DFT optimized structures of two proposed versions of the structural motifs of the active catalyst (L^{Ox})-Na-(THF)(PLA) in the PLA degradation reaction.

may cause restructuring and formation of a structure with an uncoordinated oxolanyl ring. The bond lengths of sodium with the oxolanyl oxygen are diverse at 2.43 and 2.36 Å after PLA coordination and undergo elongation after methanol incorporation to 2.50 and 2.44 Å. In the starting complex, these bonds are equally valued and amount to 2.44 Å. This effect may result in the subsequent breaking of one of the Na–O bonds and decoordination of the oxolanyl ring, which could significantly impact the activity of this compound in the depolymerization process as two catalysts could realistically participate in the process.

In summary, in each considered case, the active form of the catalyst after coordinating the PLA chain forms an eight-membered ring stabilized by intramolecular hydrogen bonds Ph/O···H/PLA. This form is clearly preferred compared to the motif of a four-membered ring (Na–O–Na–O) present in the structures of starting compounds, *i.e.*, classical sodium aminophenolates. Manipulating the steric hindrance of substituents has little impact on the stabilization of the obtained complexes with coordinated PLA; however, the benzyl substituent is the best choice from this set. An atypical result obtained for this set of sodium complexes is the stabilization of the metal-ring motif through unique coordination of substituents offering additional coordination centers for sodium ions.

The same "arrangement" is possible for ligands with either one or two such substituents. However, to form the arrangement, the involvement of one substituent is sufficient, while the other is inert, so the optimal ligand structure is two substituents, one of which has a donor atom. Models of rings for the investigated compounds of active catalysts in the PLA depolymerization process in the context of theoretical considerations are presented in Fig. 12.

Based on the standard approach and structures of sodium compounds, we would consider only models of active forms with a four-center core. However, by optimizing models of compounds coordinated with PLA, we obtained an entirely unprecedented model featuring an eight-membered metallacycle stabilized by hydrogen bonds, as well as an even more unique system of three interconnected metallacycles. The bilateral closure of the main ring by pyridyl fragments may block the

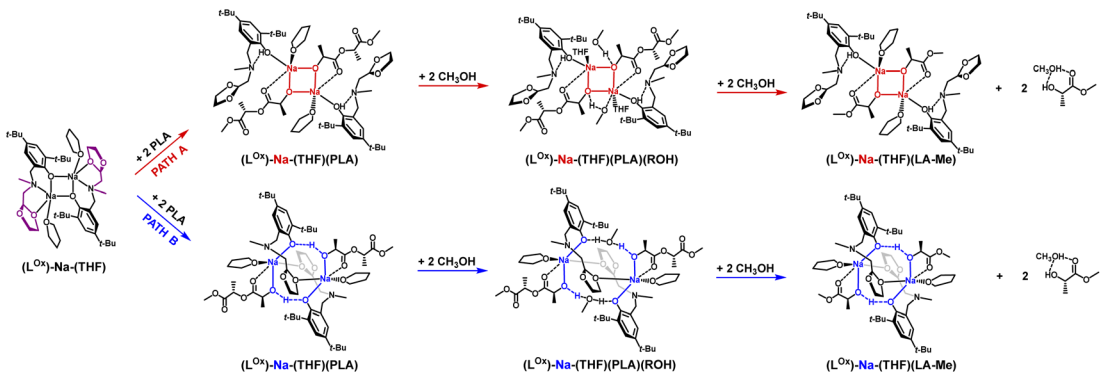

Fig. 10 Two proposed versions of the structural motifs of the active sodium catalyst (L^{Ox})-Na-(THF)(PLA) in the degradation reaction of PLA: red pathway – a four-membered motif Na–O–Na–O; blue pathway – an eight-membered ring stabilized by intramolecular hydrogen bonds Ph/O···H/PLA.

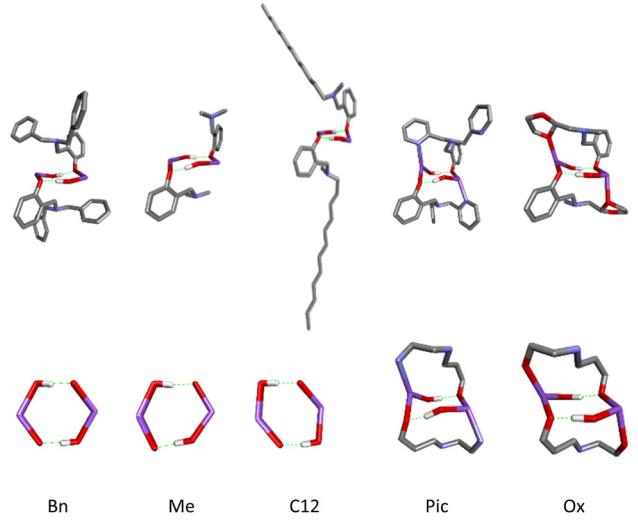

Fig. 12 Models of rings for sodium compounds active in PLA depolymerization process optimized by DFT calculations (L^R)-Na-(PLA); R = Bn, C12, Pic, Ox.

depolymerization process, forming a stable capsule. In contrast, the system with an oxolane ring exhibits a tendency for alternating decoordination, demonstrating the so-called "gorilla effect", which we previously described for magnesium compounds with this ligand. Such dynamics in solution may complicate the process, as the reaction creates inequivalent centers that not only disrupt the depolymerization process but may also transform the compound's structure into an inactive form.

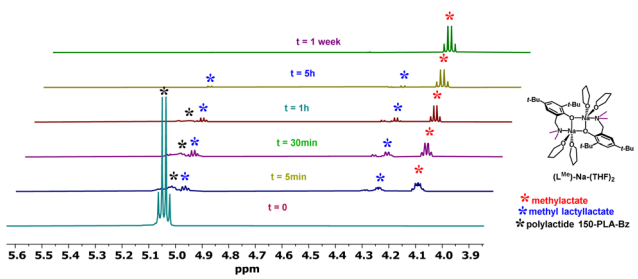

Fig. 13 The PLA degradation process in the presence of (L^{Me})-Na-$(THF)_2$ monitored by ^1H NMR (C_6D_6).

Degradation studies

The verification of theoretical studies was conducted in test depolymerization reactions in an NMR tube by sequentially introducing a sodium complex and PLA in a stoichiometry of PLA/[Na] = 1/0.5, where [Na] represents the sodium dimer.

After forming the sodium complex with PLA chains, indicated by the proton of the Ph/O···H/PLA group, methanol was added in a stoichiometry of 4 molecules of alcohol per polymer unit.

The degradation reaction of PLA was monitored using ^1H NMR spectra taken from aliquots sampled at appropriate time intervals until the disappearance of the CH group signals from PLA; an example for (L^{Me})-Na-$(THF)_2$ is shown in Fig. 13 and Table 1. Sodium compounds with steric hindrance on the amino arm (L^R)-Na-(THF); R = Me, C12 exhibit similar activity in the PLA depolymerization reaction (Table 1), degradation of PLA with 150 mers occurs after 1 hour. However, (L^{Pic})-Na forms a stable complex with PLA and shows no activity in the degradation reaction even after 7 days. This result is consistent with suggestions from theoretical studies. The formation of an additional "ring" by binding the aminophenolate ligand to two sodium centers through the phenolic oxygen and the nitrogen from the picolyl substituent effectively stabilizes the metal center, preventing the incorporation of methanol molecules and the required subsequent polymer chain transformations. Meanwhile, the (L^{Ox})-Na-(THF) complex degrades most of the PLA-150 within a few hours, and at this stage, the reaction stops Table 1. This result may suggest a modification of the compound (L^{Ox})-Na-(THF) associated with the decoordination of one of the arms forming the stabilizing ring around the eight-membered inner ring.

To verify this hypothesis, DFT studies were carried out to optimize the newly proposed structural motif, as shown in Fig. 14. The results indicate that decoordination of one arm is energetically favorable, with an energy difference of −10.3 kcal mol^{-1} (Fig. 15). Such an arrangement suggests that the polymer coordinates to both sodium centers, but only one of them can actively degrade the polymer chain (Fig. 14 and 15). Blocking the eight-membered ring on one side through the

Table 1 Depolymerization of 150-PLA-BzOH with sodium compounds [Na] and methyl alcohol

[Na]	[Na]/150-PLA-BzOH/MeOH	Time	Methyl-lactyllactate [%]	Methyl-lactate [%]	PLA [%]	Mer number of remaining PLA
(L^{Ox})-Na-(THF)	0.5/1/600	1 h	10.96	12.34	76.70	75
(L^{Ox})-Na-(THF)	0.5/1/600	7 d	13.21	16.45	70.34	70
(L^{Ox})-Na-(THF)	1/1/600	5 min	25.62	38.15	36.23	17
(L^{Ox})-Na-(THF)	1/1/600	1 h	15.34	83.65	1.01	0
(L^{Pic})-Na	0.5/1/600	1 d	3.25	1.43	95.33	100
(L^{Pic})-Na	0.5/1/600	7 d	4.12	2.04	93.85	80
(L^{C12})-Na-(THF)	0.5/1/600	1 h	15.97	26.74	57.29	25
(L^{Me})-Na-$(THF)_2$	0.5/1/600	1 h	14.95	75.79	9.25	3

Reaction conditions: CH_2Cl_2; T = 25 °C; inert atmosphere.

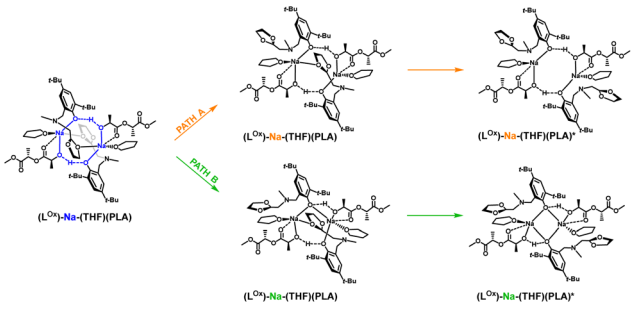

Fig. 14 Proposed version of the active catalyst (L^{Ox})-Na-(THF)(PLA) structural motif with decoordination of amine arms in the degradation reaction of PLA.

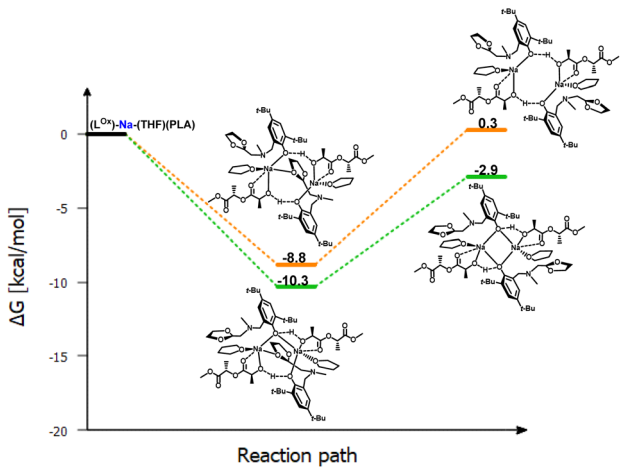

Fig. 15 Relative Gibbs free energies for DFT optimized structures of proposed version of the active catalyst (L^{Ox})-Na-(THF)(PLA) structural motif with decoordination of amine arm in the degradation reaction of PLA.

coordination of the oxolane arm allows access to only one sodium center.

Meanwhile, the results obtained from the degradation of PLA in a modified molar ratio of [Na]/PLA indicate that the polymer coordinates to only one center, forming a different structural motif which presents a more effective process. Another possible solution assumes that PLA coordination occurs sequentially through the decoordination of one arm, followed by the binding of PLA to one sodium ion. Meanwhile, the oxolane oxygen atoms coordinate to the other sodium ion. The newly proposed version of the sodium complex, optimized *via* DFT calculations with one active sodium center, is shown in Fig. 16. The addition of PLA causes the decoordination of

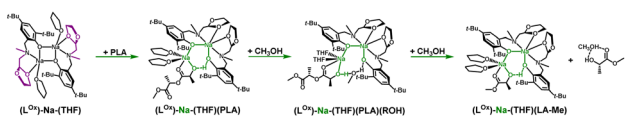

Fig. 16 Proposed version of the active catalyst (L^{Ox})-Na-(THF) structural motif with one active centre in the degradation reaction of PLA.

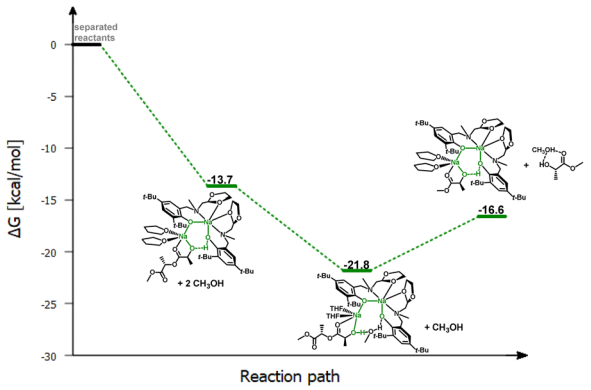

Fig. 17 Relative Gibbs free energies for DFT optimized structures of proposed version of the active catalyst (L^{Ox})-Na-(THF) structural motif with one active centre in the PLA degradation reaction.

one oxolane ring, followed by the rotation of the ancillary ligand. Consequently, coordination of the oxolane ring to the other sodium atom becomes more likely. As a result, one center is blocked by two amine arms and becomes inactive. This model is plausible; verification through energy profile analysis indicated that the proposed reaction pathway is spontaneous, as depicted in Fig. 17.

In this scenario, one of the sodium ions is privileged in the subsequent stages of the degradation reaction. In light of this suggestion, which also emerges from theoretical considerations, changing the molar ratio of the sodium complex to PLA could increase the efficiency of the degradation reaction.

Changing the reaction stoichiometry according to this modification proved to be appropriate; the degradation of 150-PLA-BzOH occurs within 1 hour. The structural motif of the active center remains the same, so the coordination environment of the sodium ion contains a coordinated PLA chain, which, through hydrogen bonding with the phenolic oxygen of the ligand, forms a bridge with the second sodium ion. However, opening the ring increases the efficiency of one center by removing blocking steric hindrance.

Substituents on the amine arm containing additional donor atoms significantly influence the structure of the active form of the catalyst after coordination with polylactide. By controlling their design, a molecular container can be formed with the polymer locked inside, preventing its depolymerization. This is how the picolyl substituent works. The same type of capsule, but with an oxolane ring, behaves differently; the blocking arm undergoes dynamic coordination and decoordination, freeing one of the active sites, and the change in reaction stoichiometry results in complete depolymerization reaction conversion.

Experimental

General materials, methods, and procedures

All reactions and operations that required an inert atmosphere of N_2 or Ar (such as those involving sodium compounds and

depolymerization reactions) were performed using standard Schlenk line apparatus and vacuum line techniques, or within a glove box (MBraun). Solvents for synthesis were purified by standard methods: *n*-hexane (HPLC, VWR), dichloromethane (HPLC, VWR), and tetrahydrofuran (THF) (HPLC, VWR) were dried and purified using Solvent Purification Systems (inert, PureSolv EN 1-7 Base). MeOH (HPLC, VWR) was distilled in an inert atmosphere before being used in degradation reactions. All chemicals were obtained from commercial sources and used without further purification: 2,4-di-*tert*-butylphenol (99%, Sigma-Aldrich), dimethylamine, dibenzylamine (97%, Sigma-Aldrich), *N*-methylododecylamine (98%, Alfa Aesar), di(2-picolyl)amine (97%, Sigma-Aldrich), 2-methylaminomethyl-1,3-dioxolane (98%, Sigma-Aldrich), formaldehyde (37% solution in H_2O, Sigma-Aldrich), sodium hydride (95%, Sigma-Aldrich).

^{1}H NMR spectra were obtained using a Bruker Avance III 500 MHz spectrometer and a Bruker Avance III 600 MHz spectrometer. Chemical shifts are reported in parts per million (ppm) relative to the residual signals of the solvent (for C_6D_6, ^{1}H: 7.16 ppm).[64]

The depolymerization experiment was carried out following the method reported in literature.[62]

Sodium complexes were synthesised according to a literature procedure.[63]

In a typical depolymerization experiment, the sodium complex and polylactide 150-PLA-BzOH in stoichiometric amounts of 0.5/1 or 1/1 (for (L^{Ox})-Na-(THF)) were dissolved in CH_2Cl_2 and stirred under an inert atmosphere of N_2 at ambient temperature. Next, MeOH was added to the stirred solution in a MeOH/PLA molar ratio of 600/1. The reaction conversion was monitored using ^{1}H NMR spectroscopy. The reaction was prepared in a glove box. For the representative procedure for the depolymerization of 150-PLA-BzOH: (L^{Ox})-Na-(THF) (0.0013 g, 0.0015 mmol), 150-PLA-BzOH (0.032 g, 0.0015 mmol), MeOH (0.036 mL, 0.9 mmol) were used.

Theoretical calculations

All structures presented in this article were fully optimized at the B3LYP-D3/6-31g(d) (hybrid density functional with D3 damping function to include dispersion) level of theory in the gas phase.[65–68] All optimizations were carried out in Gaussian16, Rev.C.O1 set of codes.[69] The vibrational frequencies were calculated to confirm that all obtained geometries are true minima since there were no imaginary frequencies. All data were analysed and visualized using the GaussView6,[70] Gnuplot[71] and Discovery Studio 3.1.[72]

Conclusions

Our comprehensive investigation into the coordination chemistry of sodium aminophenolates for the depolymerization of polylactide (PLA) has yielded significant insights into the design and application of these complexes as effective catalysts. The study meticulously examined the formation, structural characteristics, and catalytic behavior of sodium aminophenolate dimers and their larger aggregates, highlighting the crucial role of ligand design, particularly the manipulation of steric hindrances and the incorporation of donor atoms, in dictating the stability and reactivity of these coordination entities.

Key findings from our paper demonstrate that the structural motif involving a four-center core (Na–O–Na–O) is fundamental to the formation of both dimers and larger aggregates such as tetramers. This motif provides a versatile platform for the coordination of PLA, facilitating its degradation. Our theoretical DFT studies have been instrumental in identifying an energetically favorable eight-membered ring motif stabilized by intramolecular hydrogen bonds, which significantly enhances the catalytic efficiency for PLA degradation. This structural motif represents a novel paradigm in the design of sodium-based catalysts for polymer degradation, offering a more preferred pathway over traditional four-membered motifs.

Experimental validation through NMR spectroscopy and degradation studies corroborated the theoretical predictions, confirming the superior catalytic activity of complexes exhibiting the eight-membered ring structure. The study further elucidates the influence of steric factors and the presence of donor atoms on the ligand's ability to form active catalyst structures, with benzyl-substituted ligands showing optimal performance.

To sum up, our research underscores the importance of ligand design in the development of sodium aminophenolate coordination entities as powerful catalysts for the depolymerization of PLA. The findings highlight the potential of these complexes in environmental applications, particularly in the recycling of biodegradable plastics. The insights gained from this study pave the way for further exploration into the design of metal–ligand coordination systems for polymer degradation, with the aim of enhancing efficiency and specificity in catalytic processes.

Conflicts of interest

There are no conflicts to declare.

Acknowledgements

The authors would like to express gratitude to the Excellence Initiative – Research University (grant BPIDUB.4610.216.2022) for the support of this research and to the Wrocław Centre for Networking and Supercomputing (**https://www.wcss.wroc.pl**) for providing computational time and facilities.

References

1 K. Ghosh and B. H. Jones, Roadmap to Biodegradable Plastics—Current State and Research Needs, *ACS Sustainable Chem. Eng.*, 2021, **9**, 6170–6187.

2 R. Geyer, J. R. Jambeck and K. L. Law, Production, use, and fate of all plastics ever made, *Sci. Adv.*, 2017, **3**, e1700782.
3 J. Payne, P. McKeown and M. D. Jones, A circular economy approach to plastic waste, *Polym. Degrad. Stab.*, 2019, **165**, 170–181.
4 A. Samir, F. H. Ashour, A. A. A. Hakim and M. Bassyouni, Recent advances in biodegradable polymers for sustainable applications, *npj Mater. Degrad.*, 2022, **6**, 1–28.
5 M. Rabnawaz, I. Wyman, R. Auras and S. Cheng, A roadmap towards green packaging: the current status and future outlook for polyesters in the packaging industry, *Green Chem.*, 2017, **19**, 4737–4753.
6 A. Z. Naser, I. Deiab and B. M. Darras, Poly(lactic acid) (PLA) and polyhydroxyalkanoates (PHAs), green alternatives to petroleum-based plastics: a review, *RSC Adv.*, 2021, **11**, 17151–17196.
7 J. Ahmed and S. K. Varshney, Polylactides—Chemistry, Properties and Green Packaging Technology: A Review, *Int. J. Food Prop.*, 2011, **14**, 37–58.
8 T. A. Swetha, A. Bora, K. Mohanrasu, P. Balaji, R. Raja, K. Ponnuchamy, G. Muthusamy and A. Arun, A comprehensive review on polylactic acid (PLA) – Synthesis, processing and application in food packaging, *Int. J. Biol. Macromol.*, 2023, **234**, 123715.
9 V. DeStefano, S. Khan and A. Tabada, Applications of PLA in modern medicine, *Eng. Regener.*, 2020, **1**, 76–87.
10 M. S. Singhvi, S. S. Zinjarde and D. V. Gokhale, Polylactic acid: synthesis and biomedical applications, *J. Appl. Microbiol.*, 2019, **127**, 1612–1626.
11 D. da Silva, M. Kaduri, M. Poley, O. Adir, N. Krinsky, J. Shainsky-Roitman and A. Schroeder, Biocompatibility, biodegradation and excretion of polylactic acid (PLA) in medical implants and theranostic systems, *Chem. Eng. J.*, 2018, **340**, 9–14.
12 J.-M. Raquez, Y. Habibi, M. Murariu and P. Dubois, Polylactide (PLA)-based nanocomposites, *Prog. Polym. Sci.*, 2013, **38**, 1504–1542.
13 O. Dechy-Cabaret, B. Martin-Vaca and D. Bourissou, Controlled Ring-Opening Polymerization of Lactide and Glycolide, *Chem. Rev.*, 2004, **104**, 6147–6176.
14 H.-Y. Chen, J. Zhang, C.-C. Lin, J. H. Reibenspies and S. A. Miller, Efficient and controlled polymerization of lactide under mild conditions with a sodium-based catalyst, *Green Chem.*, 2007, **9**, 1038–1040.
15 L. Chen, L. Jia, F. Cheng, L. Wang, C. Lin, J. Wu and N. Tang, Synthesis, characterization of sodium and potassium complexes and the application in ring-opening polymerization of L-lactide, *Inorg. Chem. Commun.*, 2011, **14**, 26–30.
16 B. Calvo, M. G. Davidson and D. García-Vivó, Polyamine-Stabilized Sodium Aryloxides: Simple Initiators for the Ring-Opening Polymerization of rac-Lactide, *Inorg. Chem.*, 2011, **50**, 3589–3595.
17 W.-Y. Lu, M.-W. Hsiao, S. C. N. Hsu, W.-T. Peng, Y.-J. Chang, Y.-C. Tsou, T.-Y. Wu, Y.-C. Lai, Y. Chen and H.-Y. Chen, Synthesis, characterization and catalytic activity of lithium and sodium iminophenoxide complexes towards ring-opening polymerization of L-lactide, *Dalton Trans.*, 2012, **41**, 3659–3667.
18 F. M. García-Valle, R. Estivill, C. Gallegos, T. Cuenca, M. E. G. Mosquera, V. Tabernero and J. Cano, Metal and Ligand-Substituent Effects in the Immortal Polymerization of rac-Lactide with Li, Na, and K Phenoxo-imine Complexes, *Organometallics*, 2015, **34**, 477–487.
19 W.-J. Chuang, Y.-T. Huang, Y.-H. Chen, Y.-S. Lin, W.-Y. Lu, Y.-C. Lai, M. Y. Chiang, S. C. N. Hsu and H.-Y. Chen, Synthesis, characterization, and catalytic activity of sodium ketminiate complexes toward the ring-opening polymerization of L-lactide, *RSC Adv.*, 2016, **6**, 33014–33021.
20 X. Xu, X. Pan, S. Tang, X. Lv, L. Li, J. Wu and X. Zhao, Synthesis and characterization of bisphenol sodium complexes: An efficient catalyst for the ring-opening polymerization of l-lactide, *Inorg. Chem. Commun.*, 2013, **29**, 89–93.
21 D. Alhashmialameer, N. Ikpo, J. Collins, L. N. Dawe, K. Hattenhauer and F. M. Kerton, Ring-opening polymerization of rac-lactide mediated by tetrametallic lithium and sodium diamino-bis(phenolate) complexes, *Dalton Trans.*, 2015, **44**, 20216–20231.
22 K. Devaine-Pressing, F. J. Oldenburg, J. P. Menzel, M. Springer, L. N. Dawe and C. M. Kozak, Lithium, sodium, potassium and calcium amine-bis(phenolate) complexes in the ring-opening polymerization of rac-lactide, *Dalton Trans.*, 2020, **49**, 1531–1544.
23 Y. Cui, J. Jiang, X. Mao and J. Wu, Mononuclear Salen–Sodium Ion Pairs as Catalysts for Isoselective Polymerization of rac-Lactide, *Inorg. Chem.*, 2019, **58**, 218–227.
24 F.-J. Lai, C.-H. Lee, K.-H. Wu, Y.-L. Chang, Y.-C. Lai, H.-Y. Chen, S. Ding and C.-H. Lai, Ring-opening polymerization of L-lactide by using sodium complexes bearing amide as catalysts in high polar solvent, *Polym. Bull.*, 2021, **78**, 2813–2827.
25 H.-W. Ou, K.-H. Lo, W.-T. Du, W.-Y. Lu, W.-J. Chuang, B.-H. Huang, H.-Y. Chen and C.-C. Lin, Synthesis of Sodium Complexes Supported with NNO-Tridentate Schiff Base Ligands and Their Applications in the Ring-Opening Polymerization of l-Lactide, *Inorg. Chem.*, 2016, **55**, 1423–1432.
26 H.-Y. Chen, L. Mialon, K. A. Abboud and S. A. Miller, Comparative Study of Lactide Polymerization with Lithium, Sodium, Magnesium, and Calcium Complexes of BHT, *Organometallics*, 2012, **31**, 5252–5261.
27 R. Petrus and P. Sobota, Magnesium and zinc alkoxides and aryloxides supported by commercially available ligands as promoters of chemical transformations of lactic acid derivatives to industrially important fine chemicals, *Coord. Chem. Rev.*, 2019, **396**, 72–88.
28 P. McKeown, S. N. McCormick, M. F. Mahon and M. D. Jones, Highly active Mg(II) and Zn(II) complexes for the ring opening polymerisation of lactide, *Polym. Chem.*, 2018, **9**, 5339–5347.

29 J. Wojtaszak, K. Mierzwicki, S. Szafert, N. Gulia and J. Ejfler, Homoleptic aminophenolates of Zn, Mg and Ca. Synthesis, structure, DFT studies and polymerization activity in ROP of lactides, *Dalton Trans.*, 2014, **43**, 2424–2436.
30 J. Ejfler, S. Szafert, K. Mierzwicki, L. B. Jerzykiewicz and P. Sobota, Homo- and heteroleptic zinc aminophenolates as initiators for lactide polymerization, *Dalton Trans.*, 2008, 6556–6562.
31 D. Jędrzkiewicz, J. Ejfler, N. Gulia, Ł. John and S. Szafert, Designing ancillary ligands for heteroleptic/homoleptic zinc complex formation: synthesis, structures and application in ROP of lactides, *Dalton Trans.*, 2015, **44**, 13700–13715.
32 D. Jędrzkiewicz, I. Czeluśniak, M. Wierzejewska, S. Szafert and J. Ejfler, Well-controlled, zinc-catalyzed synthesis of low molecular weight oligolactides by ring opening reaction, *J. Mol. Catal. A: Chem.*, 2015, **396**, 155–163.
33 S. Soobrattee, X. Zhai, K. Nyamayaro, C. Diaz, P. Kelley, T. Ebrahimi and P. Mehrkhodavandi, Dinucleating Amino-Phenolate Platform for Zinc Catalysts: Impact on Lactide Polymerization, *Inorg. Chem.*, 2020, **59**, 5546–5557.
34 V. Piemonte and F. Gironi, Kinetics of Hydrolytic Degradation of PLA, *J. Polym. Environ.*, 2013, **21**, 313–318.
35 H. Tsuji, T. Saeki, T. Tsukegi, H. Daimon and K. Fujie, Comparative study on hydrolytic degradation and monomer recovery of poly(l-lactic acid) in the solid and in the melt, *Polym. Degrad. Stab.*, 2008, **93**, 1956–1963.
36 H. Tsuji, H. Daimon and K. Fujie, A New Strategy for Recycling and Preparation of Poly(l-lactic acid): Hydrolysis in the Melt, *Biomacromolecules*, 2003, **4**, 835–840.
37 F. Codari, S. Lazzari, M. Soos, G. Storti, M. Morbidelli and D. Moscatelli, Kinetics of the hydrolytic degradation of poly (lactic acid), *Polym. Degrad. Stab.*, 2012, **97**, 2460–2466.
38 X. Song, H. Wang, X. Yang, F. Liu, S. Yu and S. Liu, Hydrolysis of poly(lactic acid) into calcium lactate using ionic liquid [Bmim][OAc] for chemical recycling, *Polym. Degrad. Stab.*, 2014, **110**, 65–70.
39 F. Liu, J. Guo, P. Zhao, Y. Gu, J. Gao and M. Liu, Facile synthesis of DBU-based protic ionic liquid for efficient alcoholysis of waste poly(lactic acid) to lactate esters, *Polym. Degrad. Stab.*, 2019, **167**, 124–129.
40 H. Liu, R. Zhao, X. Song, F. Liu, S. Yu, S. Liu and X. Ge, Lewis Acidic Ionic Liquid [Bmim]$FeCl_4$ as a High Efficient Catalyst for Methanolysis of Poly (lactic acid), *Catal. Lett.*, 2017, **147**, 2298–2305.
41 X. Song, X. Zhang, H. Wang, F. Liu, S. Yu and S. Liu, Methanolysis of poly(lactic acid) (PLA) catalyzed by ionic liquids, *Polym. Degrad. Stab.*, 2013, **98**, 2760–2764.
42 R. Petrus, D. Bykowski and P. Sobota, Solvothermal Alcoholysis Routes for Recycling Polylactide Waste as Lactic Acid Esters, *ACS Catal.*, 2016, **6**, 5222–5235.
43 B. Nim and P. Opaprakasit, Quantitative analyses of products from chemical recycling of polylactide (PLA) by alcoholysis with various alcohols and their applications as healable lactide-based polyurethanes, *Spectrochim. Acta, Part A*, 2021, **255**, 119684.
44 F. A. Leibfarth, N. Moreno, A. P. Hawker and J. D. Shand, Transforming polylactide into value-added materials, *J. Polym. Sci., Part A: Polym. Chem.*, 2012, **50**, 4814–4822.
45 C. Alberti, N. Damps, R. R. R. Meißner and S. Enthaler, Depolymerization of End-of-Life Poly(lactide) via 4-Dimethylaminopyridine-Catalyzed Methanolysis, *ChemistrySelect*, 2019, **4**, 6845–6848.
46 H. Liu, X. Song, F. Liu, S. Liu and S. Yu, Ferric chloride as an efficient and reusable catalyst for methanolysis of poly (lactic acid) waste, *J. Polym. Res.*, 2015, **22**, 135.
47 E. M. Filachione, J. H. Lengel and C. H. Fisher, Preparation of Methyl Lactate, *Ind. Eng. Chem.*, 1945, **37**, 388–390.
48 L. D. Brake, *US Pat*, 5264614, 1993.
49 E. Cheung, C. Alberti and S. Enthaler, Chemical Recycling of End-of-Life Poly(lactide) via Zinc-Catalyzed Depolymerization and Polymerization, *ChemistryOpen*, 2020, **9**, 1224–1228.
50 X. Li, S. Gong, L. Yang, F. Zhang, L. Xie, Z. Luo, X. Xia and J. Wang, Study on the Degradation Behavior and Mechanism of Poly(lactic acid) Modification by Ferric Chloride, *Polymer*, 2019, **188**, 121991.
51 K. Janssens, W. Stuyck, K. Stiers, J. Wéry, M. Smet and D. E. De Vos, Recycling post-consumer PLA into acrylic acid or lactide using phosphonium ionic liquids, *RSC Sustainability*, 2023, **1**, 83–89.
52 G. Raia, S. Marullo, G. Lazzara, G. Cavallaro, S. Marino, P. Cancemi and F. D'Anna, Upcycling of Poly(lactic acid) Waste: A Valuable Strategy to Obtain Ionic Liquids, *ACS Sustainable Chem. Eng.*, 2023, **11**, 17870–17880.
53 C. Fliedel, D. Vila-Viçosa, M. J. Calhorda, S. Dagorne and T. Avilés, Dinuclear Zinc–N-Heterocyclic Carbene Complexes for Either the Controlled Ring-Opening Polymerization of Lactide or the Controlled Degradation of Polylactide Under Mild Conditions, *ChemCatChem*, 2014, **6**, 1357–1367.
54 E. L. Whitelaw, M. G. Davidson and M. D. Jones, Group 4 salalen complexes for the production and degradation of polylactide, *Chem. Commun.*, 2011, **47**, 10004–10006.
55 J. Payne, P. McKeown, O. Driscoll, G. Kociok-Köhn, E. A. C. Emanuelsson and M. D. Jones, Make or break: Mg(II)- and Zn(II)-catalen complexes for PLA production and recycling of commodity polyesters, *Polym. Chem.*, 2021, **12**, 1086–1096.
56 J. M. Payne, G. Kociok-Köhn, E. A. C. Emanuelsson and M. D. Jones, Zn(II)- and Mg(II)-Complexes of a Tridentate {ONN} Ligand: Application to Poly(lactic acid) Production and Chemical Upcycling of Polyesters, *Macromolecules*, 2021, **54**, 8453–8469.
57 L. A. Román-Ramírez, P. Mckeown, M. D. Jones and J. Wood, Poly(lactic acid) Degradation into Methyl Lactate Catalyzed by a Well-Defined Zn(II) Complex, *ACS Catal.*, 2019, **9**, 409–416.
58 P. Mckeown, L. Román-Ramírez, S. Bates, J. Wood and M. Jones, Zinc Complexes for PLA Formation and Chemical

Recycling: Towards a Circular Economy, *ChemSusChem*, 2019, **12**, 5233–5238.

59 J. Payne, P. McKeown, M. F. Mahon, E. A. C. Emanuelsson and M. D. Jones, Mono- and dimeric zinc(II) complexes for PLA production and degradation into methyl lactate – a chemical recycling method, *Polym. Chem.*, 2020, **11**, 2381–2389.

60 L. A. Román-Ramírez, P. McKeown, C. Shah, J. Abraham, M. D. Jones and J. Wood, Chemical Degradation of End-of-Life Poly(lactic acid) into Methyl Lactate by a Zn(II) Complex, *Ind. Eng. Chem. Res.*, 2020, **59**, 11149–11156.

61 F. Santulli, D. Pappalardo, M. Lamberti, A. Amendola, C. Barba, A. Sessa, G. Tepedino and M. Mazzeo, Simple and Efficient Zinc Catalysts for Synthesis and Chemical Degradation of Polyesters, *ACS Sustainable Chem. Eng.*, 2023, **11**, 15699–15709.

62 E. Nizioł, D. Jędrzkiewicz, A. Wiencierz, W. Paś, D. Trybuła, W. Zierkiewicz, A. Marszałek-Harych and J. Ejfler, Sodium complexes as precise tools for cutting polymer chains. Exploration of PLA degradation by unique cooperation of sodium centers, *Inorg. Chem. Front.*, 2023, **10**, 1076–1090.

63 A. Marszałek-Harych, D. Trybuła, D. Jędrzkiewicz and J. Ejfler, Scrabbling around in Synthetic Nuances Managing Sodium Compounds: Bisphenol/Bisnaphthol Synthesis by Hydroxyl Group Masking, *Inorg. Chem.*, 2020, **59**, 6895–6904.

64 H. E. Gottlieb, V. Kotlyar and A. Nudelman, NMR Chemical Shifts of Common Laboratory Solvents as Trace Impurities, *J. Org. Chem.*, 1997, **62**, 7512–7515.

65 A. D. Becke, Density–functional thermochemistry. III. The role of exact exchange, *J. Chem. Phys.*, 1993, **98**, 5648–5652.

66 C. Lee, W. Yang and R. G. Parr, Development of the Colle-Salvetti correlation-energy formula into a functional of the electron density, *Phys. Rev. B: Condens. Matter Mater. Phys.*, 1988, **37**, 785–789.

67 S. Grimme, A. Hansen, J. G. Brandenburg and C. Bannwarth, Dispersion-Corrected Mean-Field Electronic Structure Methods, *Chem. Rev.*, 2016, **116**, 5105–5154.

68 R. Ditchfield, W. J. Hehre and J. A. Pople, Self-Consistent Molecular-Orbital Methods. IX. An Extended Gaussian-Type Basis for Molecular-Orbital Studies of Organic Molecules, *J. Chem. Phys.*, 1971, **54**, 724–728.

69 M. J. Frisch, G. W. Trucks, H. B. Schlegel, G. E. Scuseria, M. A. Robb, J. R. Cheeseman, G. Scalmani, V. Barone, G. A. Petersson, H. Nakatsuji, X. Li, M. Caricato, A. V. Marenich, J. Bloino, B. G. Janesko, R. Gomperts, B. Mennucci, H. P. Hratchian, J. V. Ortiz, A. F. Izmaylov, J. L. Sonnenberg, D. Williams-Young, F. Ding, F. Lipparini, F. Egidi, J. Goings, B. Peng, A. Petrone, T. Henderson, D. Ranasinghe, V. G. Zakrzewski, J. Gao, N. Rega, G. Zheng, W. Liang, M. Hada, M. Ehara, K. Toyota, R. Fukuda, J. Hasegawa, M. Ishida, T. Nakajima, Y. Honda, O. Kitao, H. Nakai, T. Vreven, K. Throssell, J. A. Montgomery Jr., J. E. Peralta, F. Ogliaro, M. J. Bearpark, J. J. Heyd, E. N. Brothers, K. N. Kudin, V. N. Staroverov, T. A. Keith, R. Kobayashi, J. Normand, K. Raghavachari, A. P. Rendell, J. C. Burant, S. S. Iyengar, J. Tomasi, M. Cossi, J. M. Millam, M. Klene, C. Adamo, R. Cammi, J. W. Ochterski, R. L. Martin, K. Morokuma, O. Farkas, J. B. Foresman and D. J. Fox, *Gaussian 16, Revision C.01*, Inc., Wallingford CT, 2016.

70 R. Dennington, T. A. Keith and J. M. Millam, *GaussView, Version 6.1*, Semichem Inc., Shawnee Mission, KS, 2016.

71 T. Williams and C. Kelley, *Gnuplot 5.4: An Interactive Plotting Program*, 2022.

72 *BIOVIA, Dassault Systèmes, BIOVIA Discovery Studio, 3.1*, Dassault Systèmes, San Diego, 2011.